

INVESTIGATION OF MACHINABILITY OF GREEN BODIES OF SOLID CAST  
ALUMINA THROUGH THE ADDITION OF A POLY(CARBOXYLATE ETHER)-  
BASED SUPERPLASTICIZER

by

Gökay Avcı

Submitted to the Graduate School of Engineering and Natural Sciences

In partial fulfillment of the requirements for the degree of

Master of Science

Sabanci University

August, 2015

© Gökay Avcı 2015

All rights reserved

INVESTIGATION OF MACHINABILITY OF GREEN BODIES OF SOLID CAST  
ALUMINA THROUGH THE ADDITION OF A POLY(CARBOXYLATE ETHER)-  
BASED SUPERPLASTICIZER

Gökay Avcı

MAT, Master of Science Thesis, 2015

Thesis Supervisor: Assist. Prof. Özge Akbulut

Keywords: Green body machining, solid casting, superplasticizer

Abstract

The performance of a poly(carboxylate ether) (PCE)– based superplasticizer to produce machinable green bodies from suspensions of alumina with 200 nm particle size was investigated. The theoretical maximum particle packing limit was found to be 45.7 vol%. An alumina loading of 35 vol% in the presence of 1.25 wt% superplasticizer was established to be suitable for drilling and removal of significant amount of material—59% reduction in volume (77% reduction in the diameter of the green bodies) was achieved. The lathed green bodies to produce terraced structures exhibited smooth surfaces without visible cracks. All of the green bodies were sintered without a polymer burnout step. Sintered solid cast bodies shrunk  $16.1\pm 1.8\%$  at the outer diameter and  $17.5\pm 0.9\%$  at the inner diameter.

KATI DÖKÜM İLE ÜRETİLMİŞ ALUMİNA YEŞİL VÜCUTLARIN  
POLİ(KARBOKSİL ETER)- BAZLI SÜPERPLASTİKLEŞTİRİCİLER SAYESİNDE  
İŞLENEBİLİRLİĞİN İNCELENMESİ

Gökay Avcı

MAT, Master of Science Thesis, 2015

Tez Danışmanı: Yrd. Doç. Özge Akbulut

Anahtar kelimeler: Yeşil vücut seramik işlenmesi, katı döküm, süperplastikleştirici

Özet

200 nanometre tane boyutlu alumina parçacıklarından oluşan yeşil kütle seramiklerin poli(karboksil eter)- bazlı süperplastikleştiricilerle işlenebilirlik performansı incelenmiştir. Yeşil seramikler için maksimum teorik yükleme 45.7 hacim% olarak bulunmuştur. 35 hacim% alüminyum oksit yüklemeli 1.25 ağırlık% süperplastikleştirici olan parçalarda delme deneyleri ile hatrı sayılır miktarlarda madde çıkarımı—hacimde %59 düşüş (çaplarda %77 azalma) gerçekleştirilmiştir. Tornalanan yeşil seramiklerle teraslı yapılar gözle görülür çatlak oluşturmadan başarıyla işlenmiştir. Tüm yeşil seramikler polimer yakma adımı olmadan sinterlenmiştir. Sinterlenmiş seramiklerin dış çaplarında  $16.1 \pm 1.8$ , iç çaplarında  $17.5 \pm 0.9$  küçülme gerçekleşmiştir.

## ACKNOWLEDGEMENT

I would like to express my gratitude to my advisor, Özge Akbulut for her mentorship, encouragement and humility. She showed me how to work diligently and honed me to a better scientist, engineer, and person.

I would like to thank Yusuf Z. Menceloğlu and Metin H. Acar for accepting to be in my thesis jury.

Sincere gratitude is extended to following people who helped me construct this thesis:

Mehmet Ali Gülgün for providing insightful comments on alumina.

Burçin Üstbaş, Pelin Güven, Ceren Özbay and Omid Akhlaghi for being the most awesome group members.

Hasan Kurt and Meral Yüce for giving exceptional technical advice.

Canhan Şen, Güliz İnan, Melike Mercan Yıldızhan, Mustafa Baysal for being in good company and getting me uplifted and motivated.

MAT family for their altruistic efforts in sharing their experiences. I would like to especially thank to Yuda Yürüm for accepting me as a researcher in his group and introducing me to this family, Ali Rana Atılgan and Canan Atılgan for showing me the ubiquity of science, Alpay Taralp for kindling my interest towards chemistry, Clewa Ow Yang for guiding me through my career, Gözde Ince for teaching me the basics of how to conduct my own research.

My friends Selim Akın, Arda Durmaz and Melisa Maya Kumar for listening to my work and sharing their comments with enthusiasm.

My family, Naime Avcı, Lütfi Avcı and Yıldız Avcı for encouraging my path in science and supporting me no matter what. I could not have travelled this far without their love and belief.

## TABLE OF CONTENTS

CHAPTER 1 .....	12
INTRODUCTION .....	12
1. 1 Stabilization mechanisms in the suspensions of ceramic particles.....	12
1. 2 Background on superplasticizers .....	13
1. 3 Poly(carboxylate ether)-based superplasticizers.....	14
1. 4 Characterization of suspension stability .....	17
1. 5 Nanopowder processing techniques.....	19
1. 6 Green body machining parameters .....	22
CHAPTER 2 .....	28
EXPERIMENTAL.....	28
2. 1 Ceramic nanopowders.....	28
2. 2 Synthesis of the PCE-based copolymer .....	30
2. 3 Preparation of suspensions.....	30
2. 4 Rotational rheology.....	30
2. 5 Zeta potential measurements .....	31
2. 6 Mechanical characterization .....	31
2. 7 Density measurements .....	31
2. 8 Green body machining .....	31
CHAPTER 3 .....	33
RESULTS AND DISCUSSION .....	33
3. 1 Stability of suspensions .....	33
3. 2 Rheological measurements .....	34
3. 3 Mechanical characterization and machining of alumina green bodies .....	37

CHAPTER 4 .....	43
FUTURE WORK.....	43
4. 1 Robocasting .....	43
4. 2 Inkjet printing .....	44
4. 3 Hydrogen separation membranes.....	45
REFERENCES .....	47

## LIST OF FIGURES

Figure 1 Schematics that demonstrates the additional flowability enabled by the superplasticizer (retrieved from <a href="http://www.takemoto.co.jp">www.takemoto.co.jp</a> ) .....	13
Figure 2 A) poly(lignosulfonate), B) poly(naphthalene sulfonate), and C) poly(melamine sulfonate superplasticizers (retrieved from <a href="http://www.lookchem.com">www.lookchem.com</a> ) .....	14
Figure 3 Schematics of adsorption mechanisms of PCE on ceramic particles (retrieved from <a href="http://www.inkline.gr">www.inkline.gr</a> ) .....	16
Figure 4 A PCE-based superplasticizer with AA and AMPS backbone and PEG grafting(adapted from [19]) .....	17
Figure 5 Common ceramic processing techniques (retrieved from <a href="http://www.photonics.com">www.photonics.com</a> ) .....	19
Figure 6 Microcracks in gel cast alumina[30] .....	21
Figure 7 Schematics of solid casting technique a) slurry is poured inside plaster mould, b) plaster mould draws solvent via capillary action, c) additional slurry is poured until a solid body is formed, and d) solid body is taken out of the mold via dry shrinkage (adapted from <a href="http://www.tesrenewal.com">www.tesrenewal.com</a> ) .....	22
Figure 8 A) Drilling on gel casted alumina[35], B) Lathing on gel casted alumina[40], C) CNC machining on sugar bound alumina[41], D) Grooves on starch temperature induced gel [36], E) Drilled milled and lathed gel casted alumina with 5 wt% binder [42], F) Drilled and lathed urea formaldehyde gel casted sample[43] .....	27
Figure 9 Sintering profiles for alumina particles with different particle size [44] .....	29
Figure 10 Schematics of preparation of alumina green bodies.....	32
Figure 11 Effect of pH on zeta potential of the alumina suspensions in the presence of different amounts of superplasticizer.....	34
Figure 12 Viscosity of the suspensions with different alumina loading rates at $1\text{s}^{-1}$ shear rate .....	35



Figure 13 Viscosity of 35 vol% alumina suspensions in the presence of 1–4 wt% superplasticizer .....	36
Figure 14 Viscosity of suspensions with different amounts of superplasticizer at 1 s <sup>-1</sup> shear rate .....	37
Figure 15 Compressive strength and theoretical density of green bodies with different vol% alumina loading at 1.25 wt% superplasticizer.....	38
Figure 16 From left to right: green body alumina drilled by 1.1, 2, 4, 6 and 8.2 mm drill bits. The diameters of cylinders are 10.5 mm.....	39
Figure 17 A) Samples before (A) and after (B) sintering .....	41
Figure 18 Robocast green body scaffold[54].....	44
Figure 19 Inkjet print alumina before contact and after spreading on the substrate[55]	45
Figure 20 Illustration of porous hydrogen separation membranes[44].....	46

## LIST OF SYMBOLS AND ABBREVIATIONS

IEP	Iso electric point
mV	Millivolts
PMS	Poly(melamine sulfonate)
PNS	Poly(naphthalene sulfonate)
LS	Lignosulphonate
PCE	Poly(carboxylate ether)
RAFT	Reversible addition fragmentation chain transfer polymerization
AA	Acrylic acid
AMPS	2-methyl propane sulfonic acid
PAA	Poly(acrylic acid)
PEG	Poly(ethylene glycol)
PVP	Poly(vinylpyrrolidone)
PEGMA	Poly(ethylene glycol) maleic anhydride

*To my parents, past, present and  
future...*

## **CHAPTER 1**

### **INTRODUCTION**

#### 1. 1 Stabilization mechanisms in the suspensions of ceramic particles

Fine particles are subject to Van der Waals forces, which are responsible for flocculation and agglomeration in liquid media. Electrostatic interactions decay in short ranges (few nanometers) but Van der Waals forces can have their influence at a longer range (>10 nm) [1]. In order to overcome individually weak but collectively strong Van der Waals forces, different stabilization mechanisms have to be adapted. In electrostatic stabilization, the particles are shielded by the repulsion of charged stabilizers thereby providing a potential barrier that is stronger than the attractive forces. In steric stabilization, size and shape of the stabilizer provides a physical barrier which hinders particles to approach one another. Electrostatic stabilization has to offer sufficient electrical double layer length to keep particles apart whereas the polymer adlayer thickness is the main contributing factor in steric stabilization [2].

Surface area of the particles increases as size decreases and it is not possible to obtain concentrated solutions (greater than 15–20 vol%) without any stabilizers or adjustment of pH [3]. Ceramic particles can bear charge in liquid media and their charge is concerted by pH. The charge of ceramic particles in a medium can be verified by finding the isoelectric point (IEP) of the ceramic. Below IEP, the particles are mostly positively charged, at IEP the number of negative and positively charged particles are equal (thus giving a macroscopic zeta potential of 0 millivolts (mV)). Above IEP, the

particles are mostly negatively charged. The overall charge of the suspension determines the sign and amplitude of the zeta potential.

Figure 1 shows the difference between a plasticizer and a superplasticizer—plasticizer imparts malleability to ceramic powders, whereas superplasticizer provides flowability.

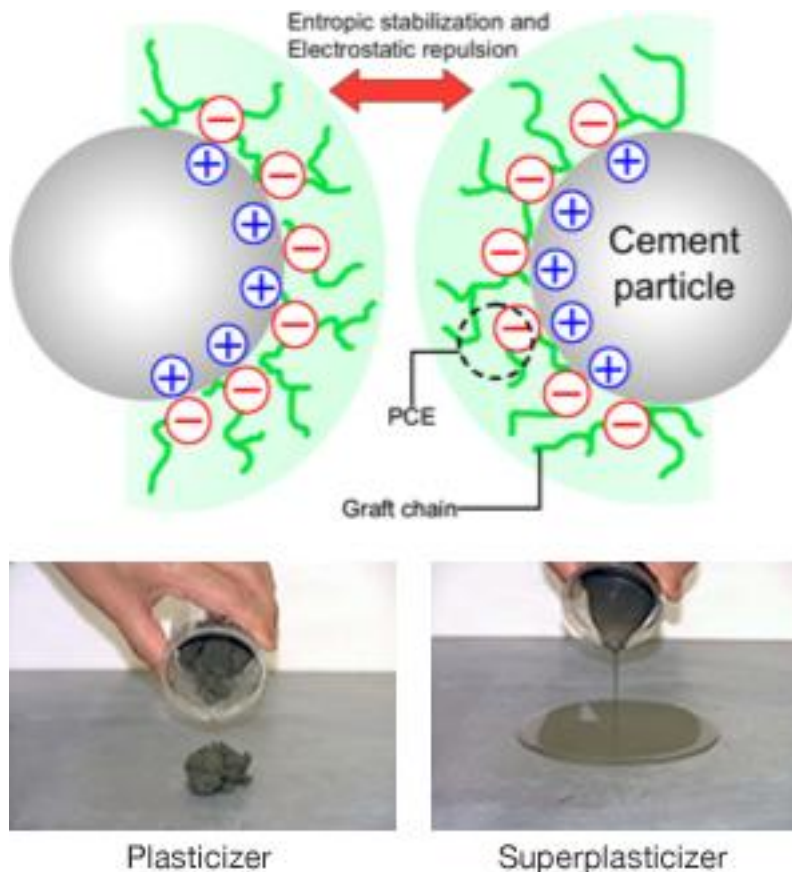


**Figure 1 Schematics that demonstrates the additional flowability enabled by the superplasticizer (retrieved from [www.takemoto.co.jp](http://www.takemoto.co.jp))**

## 1. 2 Background on superplasticizers

Superplasticizers are polymers made out of charged moieties which provide stabilization in a suspension. Superplasticizers are utilized as rheology modifiers to prevent agglomeration of particles through flocculation. Poly(melamine sulfonate) (PMS) and poly(naphthalene sulfonate) (PNS) are among first superplasticizers which provide stabilization through their charged hydroxyl sulfonate and carboxylate groups (electrostatic stabilization) as well as their high molecular weight (steric stabilization) [4,5]. PNS and PMS were both designed to offer flowability and prevent slump loss in

cement slurries. Lignosulphonates (LS) as superplasticizers have been utilized to provide concentrated alumina suspensions in water [6]. LS have been shown to provide stabilization in kaolin and silicon nitride systems at high pH without extensive adsorption [7]. Figure 2 demonstrates the chemical structure of PNS, PMS, and LS. Carboxyl, hydroxyl, and sulfonate groups mediate the interaction of superplasticizer with ceramic particles. Although PNS, PMS, and LS were extensively used in cement industry to achieve better dispersions, they were still not effective in reducing slump loss. Slump loss determines the reduction in flowability of cement slurry after certain amount of time [8]; therefore it is a reliable parameter to examine the stability of cement particles against agglomeration and flocculation.

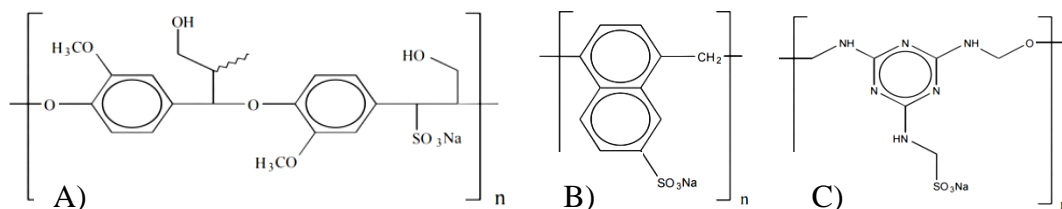


**Figure 2 A) poly(lignosulfonate), B) poly(naphthalene sulfonate), and C) poly(melamine sulfonate superplasticizers (retrieved from [www.lookchem.com](http://www.lookchem.com))**

### 1.3 Poly(carboxylate ether)-based superplasticizers

Poly(carboxylate ether) (PCE)-based superplasticizers provide exceptional slump loss retaining abilities which is related to their better adsorption profiles and stability compared to other superplasticizers. Although PCE superplasticizers were designed for cement industry, they can be used to prepare concentrated and flowable solutions of ceramics as well.

Linear PCE with active groups and short side chains have gained attention due to tailorability of its chemical structure, active group type, and frequency[9]. Although PCEs were commonly used as superplasticizers, the fundamentals of how they interact with inorganic particles were poorly understood. Early synthesis of PCE resulted with broad polydispersity thus the effect of chain size could not be investigated without

purification through chromatography columns. Advanced synthesis techniques such as reversible addition fragmentation chain transfer polymerization (RAFT) and living polymerization enabled control over poly dispersity index which catalyzed PCE research [10].

PCE-based superplasticizers can be tailored by changing, i) the length and frequency of side chains, ii) degree of polymerization, iii) monomers of backbone, and iv) monomer feed ratios [11]. Different modifications led to utilization of different types of PCE superplasticizers. Poly(acrylate) salts [12], poly(methacrylates) with carboxylic or sulfonic anions with ammonium cations [4], terpolymers with acrylic acid, acrylamide, and vinylpyrrolidone [13] have been used in preparation of concentrated ceramic pastes to, enhance flowability of these suspensions. Through the design of superplasticizers, the effect of different functional groups and structures were investigated. Marco, *et al.* proposed that linear PCE showed better dispersing abilities than sodium poly(alkyl sulfonate) with raw porcelain gras [14]. Zhou, *et al.* investigated the effect of homoacrylate, copolyacrylate, and multiacrylate of modified PCE on raw porcelain gras and suggested that the multipolymer with more charge density had achieved higher ceramic loadings and finer dispersability [9]. These findings underscore the configuration and the way the polymers adsorb on ceramic particles is crucial to elucidate rheology of ceramic slurries.

The configuration of superplasticizers determines their adsorption behavior. There have been different stable configuration modes reported such as mushroom like, brush, and cake [8]. Bowman, *et al.* found that pH of the suspension changed the configuration of poly(acrylic acid) on alumina particles, at pH higher than 9, the polymer chains assumed random coil configuration whereas at pH lower than 9 the chains assumed mushroom configuration which essentially provided increased stability [15]. Many conformation modes can be present through the slurry as illustrated in Figure 3 and these modes determine the adsorption and surface coverage behavior of polymers on nanopowders. In PCE superplasticizers, the sulfonate and carboxylic backbone functional groups compete to bind on alumina surfaces while PEG side chains protrude towards the solution.

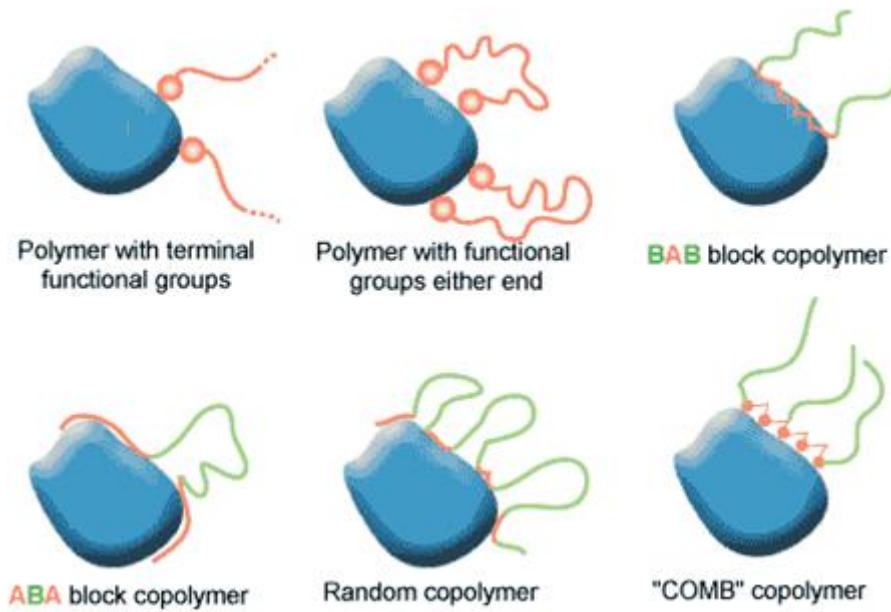


**Figure 3 Schematics of adsorption mechanisms of PCE on ceramic particles (retrieved from [www.inkline.gr](http://www.inkline.gr))**

Bouhamed, *et al.* investigated the adsorption behavior and electrokinetic properties of alumina particles with statistical and diblock PCE architectures. Block copolymers provided lower viscosity profiles compared to statistical architectures and this finding was supported by a thicker adlayer found in block copolymers [16].

Palmqvist, *et al.* compared dispersion mechanisms of PAA, LS, and a comb PCE superplasticizer on alumina particles. PAA and LS were able to reach higher dispersion rates; yet, the same alumina vol% was achieved by lesser amounts of PCE-based superplasticizer. In terms of providing higher loading suspensions, PAA and LS performed better than PCE superplasticizers [17].

Akhlaghi, *et al.* provided a systematic study on rheological properties of a PCE copolymer synthesized with acrylic acid (AA), (2-methyl propane sulfonic acid) (AMPS), and poly(ethylene glycol) (PEG) on 200 nm alumina particles. All of monomer feed ratios showed high zeta potentials in a wide pH range indicating the stabilization efficiency induced by the copolymer. [18]. Figure 4 demonstrates the chemical structure of the superplasticizer used in this work where acrylate and AMPS backbone is grafted with PEG side chains.



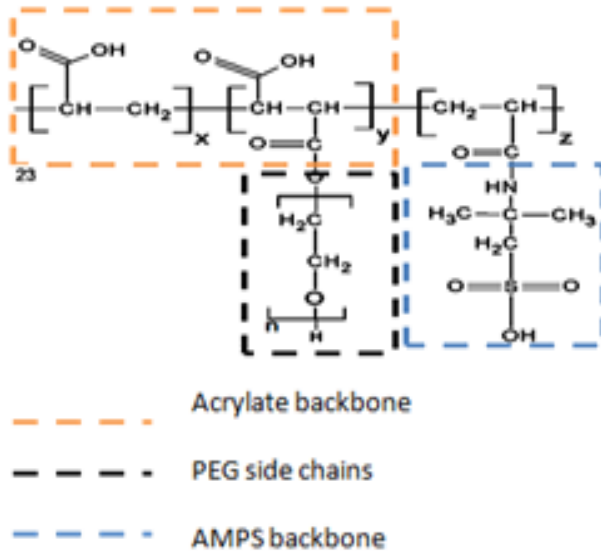


**Figure 4 A PCE-based superplasticizer with AA and AMPS backbone and PEG grafting(adapted from [18])**

#### 1. 4 Characterization of suspension stability

The dispersing ability of a rheology modifier depends on i) molecular weight, ii) pH, iii) dispersed particle size, and iv) depletion interactions. The rheological properties of the suspensions and maximum particle loading are interconnected properties of ceramic nanopowder processing [19]. As particle loading increases, the total amount of particles in the suspension also increases which hinders flowability. An important objective for ceramics processing is to attain maximum particle loading while retaining flow properties in the processing window.

Nanopowders of ceramics were commercially produced as early as 1980s but their application was limited as they could not be readily incorporated into traditional ceramic processing. In traditional ceramic slip casting with micron sized particles, the average viscosity increases as particle size decreases since the number of bonds between particles per unit volume increases. For particles lower than 1 micron size, pseudoplastic behaviour is observed which means the shear stress decreases dramatically with increasing shear rate [20]. Traditional processing parameters used for micron sized particles cannot be directly adapted to nanopowders due to this pseudoplastic behavior. New design parameters have to be determined to process nanopowders with superplasticizers.

The viscosity of suspension is crucial both for dry and wet processes, in the former, viscosity of binders determine the compactness of powders as more pressure is applied, in the latter, viscosity both determines whether the slurry is slippable and also particle packing during water removal phases. Green body packing is increased with well dispersed and highly loaded ceramic suspensions. Cesarano, *et al.* worked on suspension of 0.1–0.2 micron alumina particles dispersed with PAA and reported that the viscosity reached a minimum at the isoelectric point of alumina, but sharply increased with minimal deviations from this pH [21]. Green body packing is also affected by the size of the particles. Tallon, *et al.* systematically investigated the effect of particle size on the packing density of slip cast alumina bodies. 190 nm particles provided the highest green densities and sintered densities compared to experiments with 44 nm and 600 nm particle size [3]. Acosta, *et al.* used 0.48 micron alumina powders dispersed with poly(methacrylic acid) ammonium salt just above the IEP of alumina and provided depletion interactions with the addition of PVP where over 50 vol% loadings were obtained. The flowability of the slurry was modified by altering the molecular weight of PVP [22]. Bouhamed, *et al.* investigated dispersibility of 0.4 micron sized alumina powders with polycarboxyl ether superplasticizers from various synthesis routes; 30 vol% suspensions were used and zeta potentials which were negative through a large pH range were obtained [16].

Providing higher suspension loadings with nanopowders is difficult due to higher surface area which amplifies Van der Waals forces. Particles with moderate loadings can be stabilized with electrostatic repulsions. This approach is insufficient when higher loadings are present; the crowded particles are forced within each other mechanically as slurry is mixed. This compression leads to flocculation where potential barrier for electrostatic repulsions are breached by Van der Waals forces. Steric repulsions are necessary to achieve particles with higher loadings. The dispersion with steric stabilizers compress the stabilizers but due to unfavorable energetics that require conformation change, destabilization does not occur if there is a high surface coverage of polymers over the ceramic particles. The dispersion medium has to be a good solvent for the stabilizer such that interpenetration of particles is unfavorable and the segments protrude into the external solution. PAA has been found to be a good steric stabilizer since the polymers assume an expanded configuration in water [23]. This effect can also

be seen in polymers grafted with PEG side chains with different classes of superplasticizers, where length and frequency of the peg side chain promotes dispersion stability.

### 1. 5 Nanopowder processing techniques

In ceramics processing, particle consolidation techniques determine the final structure of the cast body. Ceramics can either be processed in a wet state or a dry state. In dry processing techniques nanopowders are needed to be deaired before applying proper force. In the wet state, without any additives, the particles tend to coagulate and form flocs which have a lower effective density than particles on their native state. In order to provide stable suspension that does not form any flocs and does not coagulate, plasticizers and superplasticizers can be incorporated into the slurry.

Figure 5 shows various processing techniques such as powder making, injection molding, green forming and shaping, slip casting, densification and heat treatment, grinding and polishing. Ceramic processing can be separated into three main groups: i) powder consolidation, ii) firing/sintering, and iii) post-sintering operations.

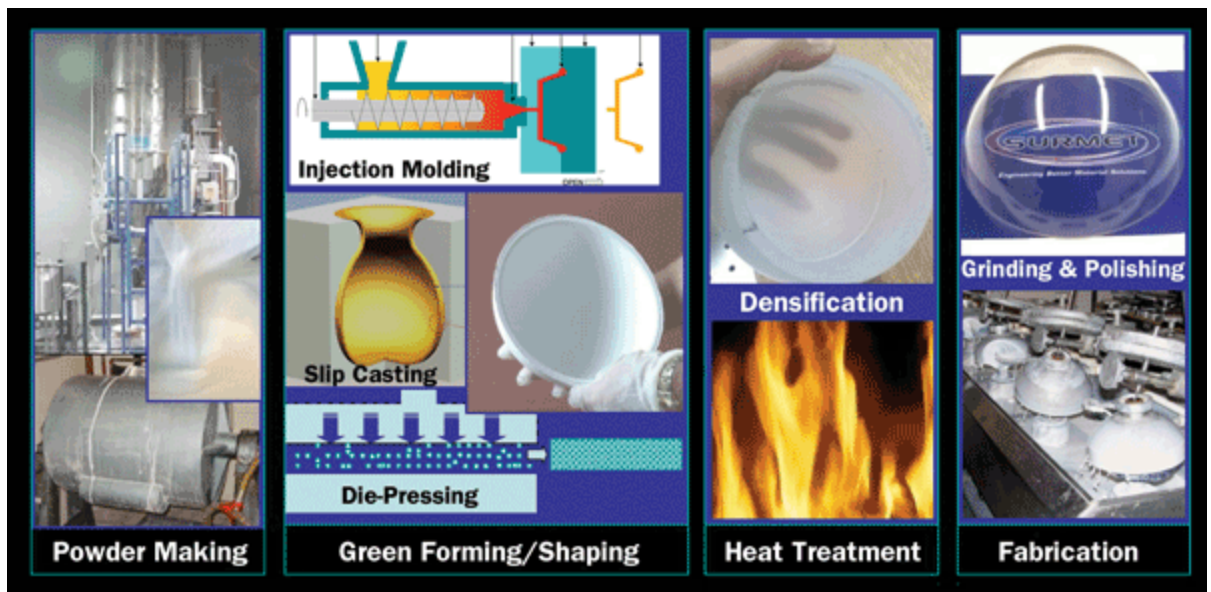
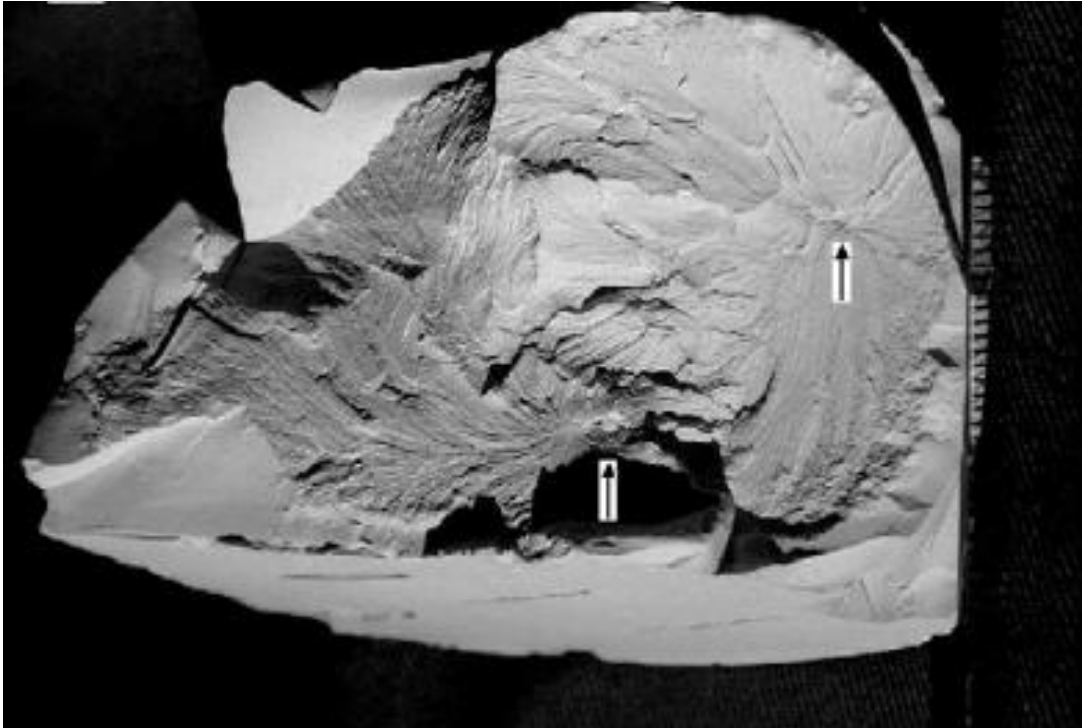


Figure 5 Common ceramic processing techniques (retrieved from [www.photonics.com](http://www.photonics.com))

Liquid-based processing methods provide an alternative to powder pressing. Liquid routes can produce green bodies with more uniform binder distribution with the ability to form different geometries other than cylindrical pellets and minimization of density gradients imminent in dry routes [24].

Gel casting is a wet green body production technique where monomers and solvent are mixed with ceramic powders and polymerized in a mold [25]. Green bodies produced with gel casting have binder contents of 4–10 wt% and green strengths that are higher than many common net-shape processing techniques [26]. Although high green strengths are achieved, reproducibility needs further improvements. Figure 6 illustrates the microcrack formation due to inhomogeneous cross-linking which reduces mechanical strength and reliability. Monomers and crosslinkers used for gel casting are highly toxic. There are efforts to produce non-toxic monomers but they fail to achieve the strength values produced by traditional gel casting [27]. The polymerization reaction is highly oxygen sensitive thus the process must be carried out in an inert atmosphere which complicates the mass production routes. Only a limited amount of chemistries are available for the current gel casting methods thus limiting the flexibility for process design. The excess slurry cannot be recycled when the slurry crosslinks, eliminating the ability to recast poor pieces [28].



**Figure 6 Microcracks in gel cast alumina [29]**

Another approach is to adapt thermo reversible gel casting in which the monomers are replaced by a polymer that provides a temperature driven physical gelation. This technique eliminates the oxygen sensitivity and enables the recapturing of miscasting but further narrows down the limited choice of monomers [30].

High amounts of binder (40–50 wt% to that of ceramic powders) is used to make a flowable ceramic polymer mixture without any solvent. The large amount of binders in injection molding requires careful and slow binder burnout to prevent any cracking in the ceramic body. Injection molding requires one dimension to be less than 3 cm in order to consolidate the particles together thus essentially limiting the application of this technique to thin objects [31].

Tape casting is an industrially important process since thin tape cast ceramic are used in electronic substrates and sensors. A ceramic slurry is slowly cast into a thin sheet, tensile stresses are brought if the drying shrinkage is large thus measures are taken to

minimize shrinkage. Homogenous tapecasting can be accomplished by using a casting suspension with high solid loadings.

Slip casting is a traditional ceramic formation process where ceramic powders are dispersed in a liquid medium to produce a suspension. As a variation of slip casting technique, in solid casting technique a) slurry is poured inside plaster mould, b) plaster mould draws solvent via capillary action, c) additional slurry is poured until a solid body is formed, and d) solid body is taken out of the mold via dry shrinkage(Figure 7) [32]. The homogenization and the rheological behavior of the suspensions play an important role in the microstructure and mechanical properties of the body [33]. In order to obtain a dense and homogenous green body the slurry should have a high solid content and good dispersion abilities [34]. Through optimization of binder and dispersant ratios, the stability and integrity enables slip cast bodies with minimal defects [35].

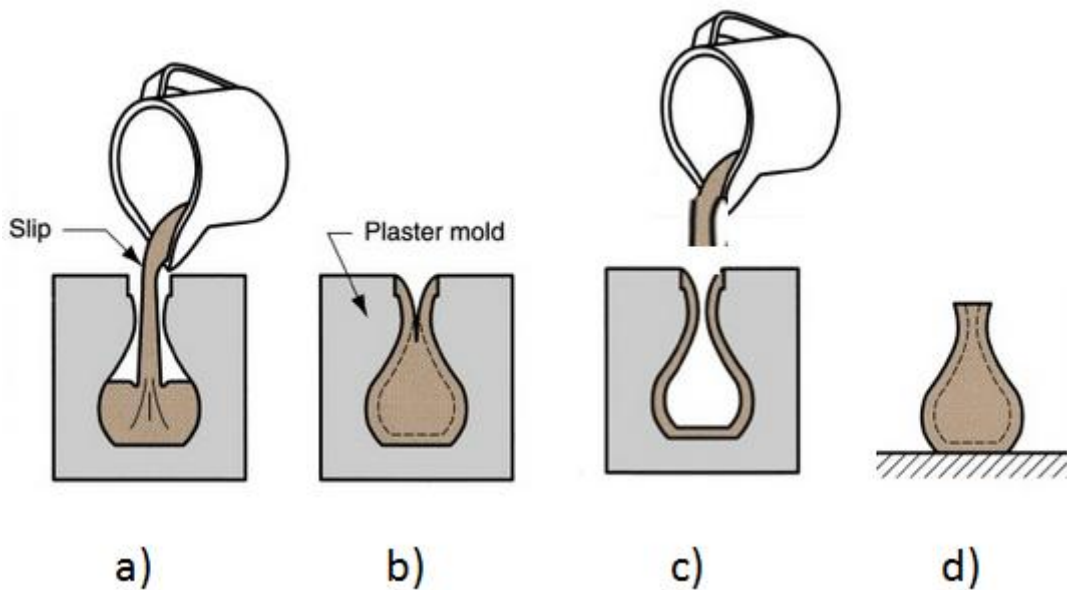


**Figure 7 Schematics of solid casting technique a) slurry is poured inside plaster mould, b) plaster mould draws solvent via capillary action, c) additional slurry is poured until a solid body is formed, and d) solid body is taken out of the mold via dry shrinkage (adapted from [www.tesrenewal.com](http://www.tesrenewal.com))**

## 1. 6 Green body machining parameters

To machine green body ceramics, i) binder burnout, ii) material removal, iii) machining mode, iv) tooling speed parameters, v) compressive strength, vi) hardness, and vii) packing rate of green body have to be considered.

*Binder burnout:* The binder burnout must be carried according to the properties of the polymer used. A TGA curve can be used to determine the time and temperature required to burn the binder without producing cracks in the green body [36]. As a rule of thumb, adding less amount of binder reduces or even eliminates binder burnout routes. As the binder amount is increased, the removal process has to be slower and more delicate to prevent catastrophic failure. The size of the material is also a crucial aspect; sintering bigger materials will require greater measures to achieve a uniform structure. The ceramic particles can be mixed with very high amount of polymers and can be extruded to a mold. This method was used originally and very slow binder burnout had to carry out in order to prevent fracture of the material. Gel casting provided a strong alternative to this traditional method and became the golden standard to produce machined green bodies. In gel casting, the polymer that has to be removed has been reduced from 50 wt% to 10-15 wt% compared to extrusion protocols. Eliminating the binder burnout would substantially benefit the green body machining saving both time and the amount of expensive additive polymers [29].

**Material Removal:** During machining the ceramic particles produce flakes rather than chips which is common in metal machining. Due to this property, the machined part of the ceramic has to be effectively removed [37]. The excess material may contribute to internal stress buildup and premature fracture of the green product. It may also lead to wearing of tool wear due to increased contact between abrasive ceramics and the machining tools.

**Machining modes:** Grinding, drilling, surface finish, steel carbide tooling, diamond coated tooling are commonly used modes to machine green samples [38].

**Tooling speed parameters:** Tooling speed varies between different modes. Using higher speeds increases material removal rates as well as the amount of force that the material has to withstand. Using high tooling speeds (greater than 1000 rpm) will also increase tooling wear rates and provoke a need to replace machining tools earlier than possible [27].

Compressive strength: Using PVA alone produces weak green bodies with compressive strengths lower than 2 MPa [29]. Tensile and shear forces act upon different regions of the material through the course of desired object. Due to this phenomenon, creating objects with thin walls and intricate structures has been a challenge in green body machining. In our work we were able to drill green bodies with thin walls which indicate the strength of the binding ability of our superplasticizer.

Hardness: Gel cast materials with compressive strengths greater than 100 MPa can be achieved by adding high amounts of binders (up to 15 wt%) which reduces hardness of the green body [27]. Machining green bodies with high strength and low hardness produces micro cracks in the structure thereby eliminating the possibility of drilling mode. We experienced that higher alumina loadings resulted in lower strain rates upon ultimate compressive strength thereby this protocol had to be optimized.

Green body theoretical density: The packing of the green body affect many aspects of green machining. As the particles are packed closer, the compressive strength is usually higher with compact structure. The microstructure homogeneity is also linked with green body packing rate where a finer microstructure produces a smoother packing [34]. The packing ratio also determines the maximum sintered density for a specific temperature/time. As the particle gets denser it shrinks. The shrinkage is also oriented by the green body packing rate where higher packing is correlated with lower shrinkage values. Providing lower shrinkage values reduces the probability of fractures and defects through sintering in complex parts.

Table 1 summarizes advantages and disadvantages of each technique. Gel casting was developed as an alternative to injection molding due to very long binder burnout times and requirement of careful and slow binder burnout step. Slip casting and pressured slip casting can be provided as a strong alternative for gel casting technique but the major drawback of slip casting technique has been the deficiency of high strength green bodies. In our work, we propose a new superplasticizer that can provide a sufficient green strength and aims to fill this strength gap for slip casting technique.



**Table 1 Ceramic consolidation techniques and their advantages and disadvantages.**

**Adapted from gelcasting, the handbook of ceramic engineering[39]**

Property	Gel casting	Slip casting	Injection molding	Pressure casting
Molding time	5–60 minutes	1–10 hours	10–60 seconds	10 minutes–5 hours
Strength (dried)	Very high	Low	N/A	Low
Mold materials	Metal, glass, polymer, wax	Plaster	Metal	Porous plastic
Binder burnout	2–3 hours	2–3 hours	7 days	2–3 hours
Mold defects	Minimal	Minimal	Significant	Minimal
Maximum part dimension	> 1 meter	> 1 meter	About 30 cm, 1 dimension must be $\leq 1$ cm	About 1 meter
Warping during drying/binder burnout	Minimal	Minimal	Possible be severe	Minimal

## 2. 2. Parameters of on green machined alumina ceramics

In Figure 8, previous work on green body machining has been analyzed.

- A) Warping was prevented by using a controlled humidity chamber. 3mm holes are drilled on gel cast samples. The samples were sintered up to 97% of theoretical density of alumina [34].
- B) Bimodal distribution of alumina particles with particles sizes of 280 nanometers and 3.4 microns were used. A classical gel casting with acryl amide and dimethacrylate monomer was modified with addition of PEG chains of 400 units

and 6000 units long. Green body strengths varied between 2 to 25 MPa depending on the binder amount. Lathing drilling and milling was performed without major damage to the samples [40].

- C) 700 nanometer sized alumina particles were dispersed in poly(maleic acid) to produce 55 vol% loaded slurries with 3 wt% sugar as binder. The slurries were cast into 24 well plates and a tooth model was fabricated via CNC machining [41].
- D) 4 micron sized alumina was gel cast with acryl amide and peg diacrylamide monomers. Flexural strength values up to 10 MPa were obtained [35].
- E) Acrylic acid was used to prepare green bodies that can be drilled, lathed and milled. With 5 wt% binder, 6 MPa green body strengths were observed. Interestingly an increase of binder content from 5 wt% to 10 wt% increased green body strength while reducing the green density. This work was shown as an alternative to gel casting techniques where humidity chambers were necessary to dry the samples. Due to high wt% polymers inside gel casted samples, drying without humidity chambers causes warping and cracking through the sample. 11.5 MPa green body strengths with addition of 10 wt% binders were achieved [42].
- F) Urea formaldehyde was cross linked in PAA media. The binder composition with 1:1 ratio of acrylic and urea formaldehyde showed the best compressive strength at 7 MPa. Theoretical densities greater than 97% were achieved on 1550°C 2 hour sintered bodies. Recessed steps were made by lathing and hole was made by drilling [43].

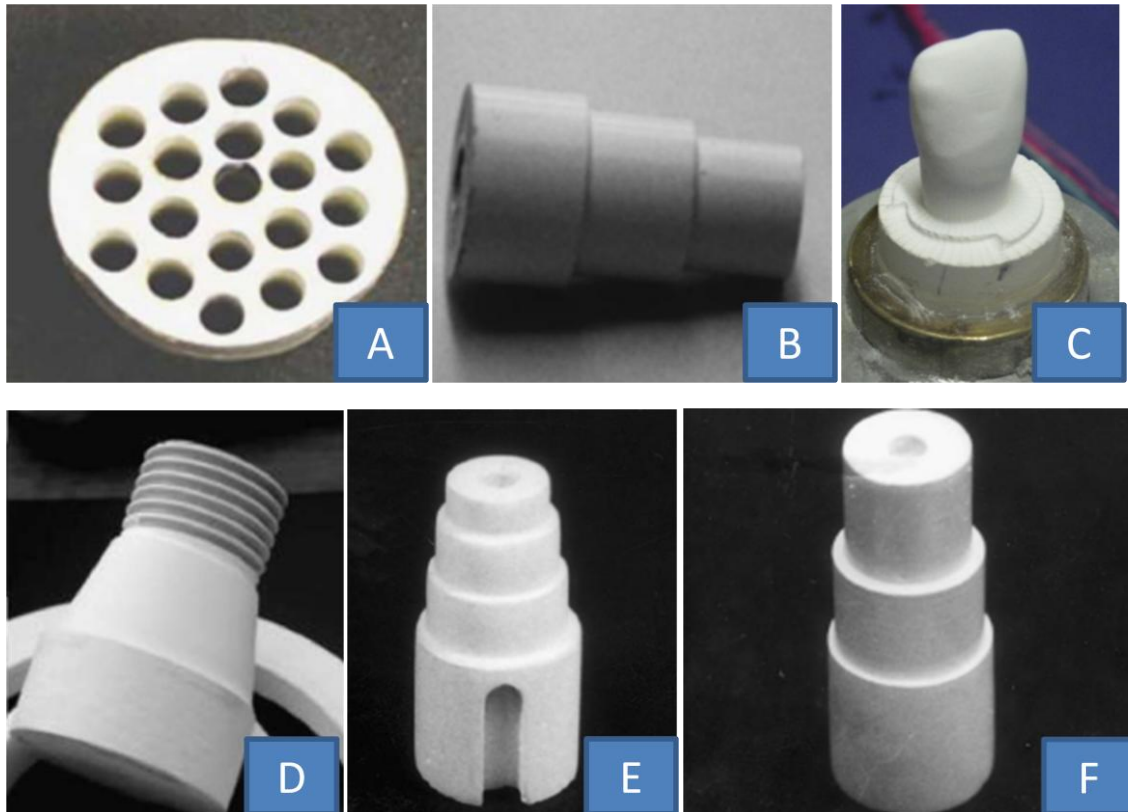


**Figure 8** A) Drilling on gel cast alumina [34], B) Lathing on gel cast alumina [40], C) CNC machining on sugar bound alumina [41], D) Grooves on starch temperature induced gel [35], E) Drilled milled and lathed gel cast alumina with 5 wt% binder [42], F) Drilled and lathed urea formaldehyde gel cast sample [43]

## CHAPTER 2

### EXPERIMENTAL

#### 2. 1 Ceramic nanopowders

Carron, *et al.* empirically determined the optimal particle size to achieve best packing of nanopowders with solid casting technique and concluded that nanopowders with 100–300 nm size provided the best packing compared to smaller and larger powders[3]. Therefore, in this work we chose to work with alumina nanopowder (AKP-50, Sumitomo Chemicals, Japan) with average particle size of 200 nm, purity of > 99.99%, and BET surface area of 10.9 m<sup>2</sup>/g..

Alumina is processed from bauxite via calcinations [44]. Alumina can be produced in many different particle sizes and also in different phases of alumina ( $\alpha$  phase,  $\beta$  phase and  $\gamma$  phase).  $\alpha$  phase is stable at room temperature whereas  $\beta$  and  $\gamma$  phase are metastable. Metastable phase alumina were shown not to sinter into dense bodies thus we used  $\alpha$ -alumina for our experiments [3].

As shown in Figure 9, the sintering temperature of  $\alpha$ -alumina decreases as particle size decrease. This behavior is directly related to the chemical potential of nanopowders. Nanopowders have higher surface areas thus chemical potential of nanopowders are much higher than micron sized particles. High chemical potential/surface area reduces the activation energy to initiate necking between nanopowders thus reducing the sintering temperatures both results in saving energy and refractory maintenance costs.

Nanopowder processing provides a wider control on final particle size compared to micron sized powder processing techniques [45].

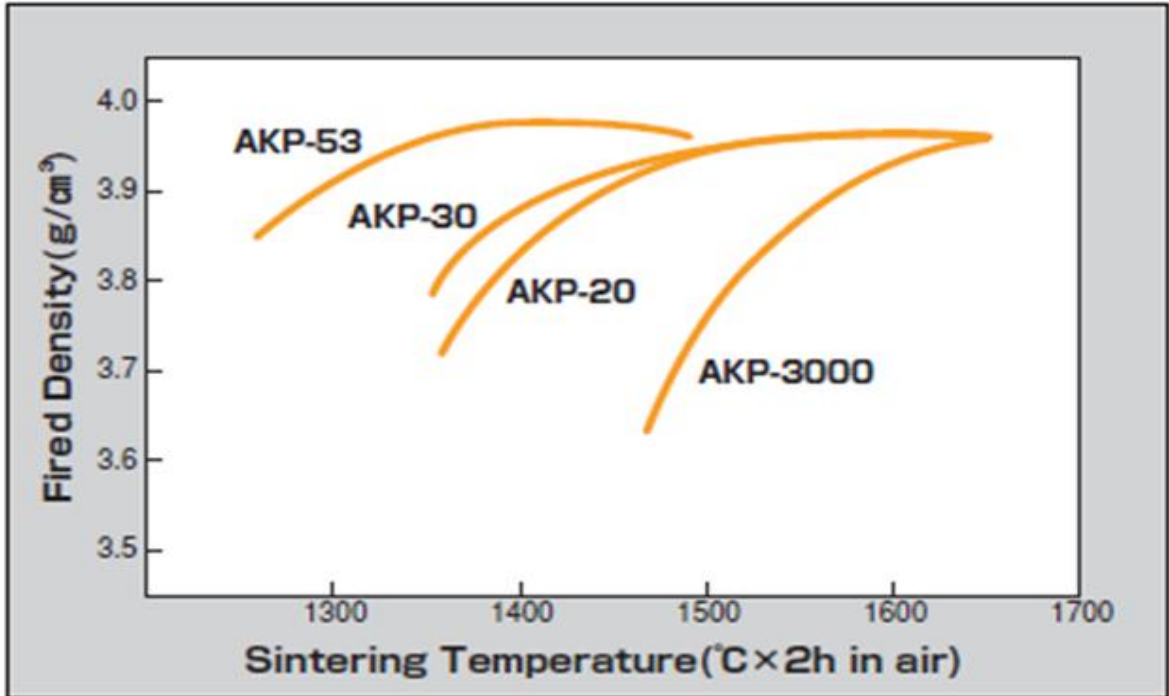


**Figure 9 Sintering profiles for alumina particles with different particle size [44]**

Although control over particle size is desired, it comes with the cost of homogeneity. Due to high surface areas of nanopowders, more polymers need to adsorb on the available surfaces to provide flowability. Viscosities of nanopowders are higher than micron sized powders. There is a need for flowable nanopowder slurries which can provide well packing of green body.

Smaller grain size results in higher strength and toughness. This behavior can be explained by the Hall-Petch relationship. Nanograins prevent intergrain slips which provide higher strength and toughness to the material. Smaller particle sizes provide a faster grain growth rate with lower activation energy, thereby reducing the sintering temperature. In order to harness this kinetic barrier difference between grain boundary diffusion and grain boundary migration, Chen, *et al.* devised a simple two step sintering technique. In this technique the particles are sintered at standard temperatures briefly

and then the temperature is reduced 300 °C for a longer time period. This approach prevents grain growth while providing sufficient energy for complete sintering [45]. Uniform and controlled porosity is desired for advanced applications which can be accomplished by understanding the behaviour of nanopowder alumina.

## 2. 2 Synthesis of the PCE-based copolymer

The comb-type PCE superplasticizer, hereafter referred as superplasticizer, is composed of acrylic acid (AA), 2-acrylamido-2-methylpropane sulfonic acid (AMPS) and maleic anhydride modified poly(ethylene glycol) with molecular weight of 1000 g/mol (PEGMA). The superplasticizer was synthesized through a method described by Salami and Plank[46]. The ratios of the monomers were 25/25/1 (AA/AMPS/PEGMA) and the reaction was carried out at pH 8. These conditions were chosen based on the performance of this copolymer in our previous work compared to other copolymers that are synthesized with different monomer ratios and different pH values.

## 2. 3 Preparation of suspensions

Suspensions of 30–40 vol% alumina particles and different amounts of copolymers were prepared using an ultrasound probe (Vibra Cell 75041, Bioblock Scientific) in pulse mode (2 seconds on, 2 seconds off) for 4 minutes to break soft agglomerations. The suspensions were stirred for 24 hours in a capped container to prevent evaporation. Figure 10 illustrates the protocol used for our work.

## 2. 4 Rotational rheology

The rotational rheology was conducted in Anton-Paar MCR 302 rheometer with cone-plate geometry of 50 mm/2° and a gap size of 0.208 mm. After loading of each sample, a thin layer of low-viscosity paraffin oil was employed around the outer edge of the platens to protect the sample from evaporation. Temperature was set to 25 °C and the shear rate ranged from 0.1 to 1000 s<sup>-1</sup>.

## 2. 5 Zeta potential measurements

Zeta potentials of the suspensions were monitored by using Zetasizer nanoseries (Malvern Instruments, Ltd.). After addition of 0.001 wt% alumina particles to superplasticizer solutions and 1 hour of stirring, pH of the mixture was adjusted in between 2–12. Subsequently, six measurements with at least 20 cycles were performed at 25 °C and the average value was reported.

## 2. 6 Mechanical characterization

The compression tests on green bodies were performed with Zwick/Roell Z100 universal testing machine according to ASTM 773 standard. All suspensions were cast in homemade gypsum molds (3/4 vol/vol gypsum to water ratio) to obtain full solid bodies with a diameter of 11 mm and a height of 15 mm. All samples were de-molded after 24 hours and then dried at 70°C for 24 hours. Each experiment was repeated 5 times.

## 2. 7 Density measurements

AccupycII-1340 gas pycnometer was used to measure theoretical densities of green body alumina samples. Before measurement, each sample was covered with silicone oil preventing gas penetration through open pores.

## 2. 8 Green body machining

The samples were drilled 6 mm deep and with up to 8 mm wide holes using conventional high speed steel drilling heads. Samples did not fail during machining. Drilling deeper than 4–5 mm without getting rid of excess material, initiated internal cracks. Machined samples were sintered at 1500°C for 2 hours with a heating rate of 5°C/min with no binder burnout step. 500-900 rpm was used for drilling and 700-1200 rpm for lathing. For shrinkage rates an average of 5 samples were reported.

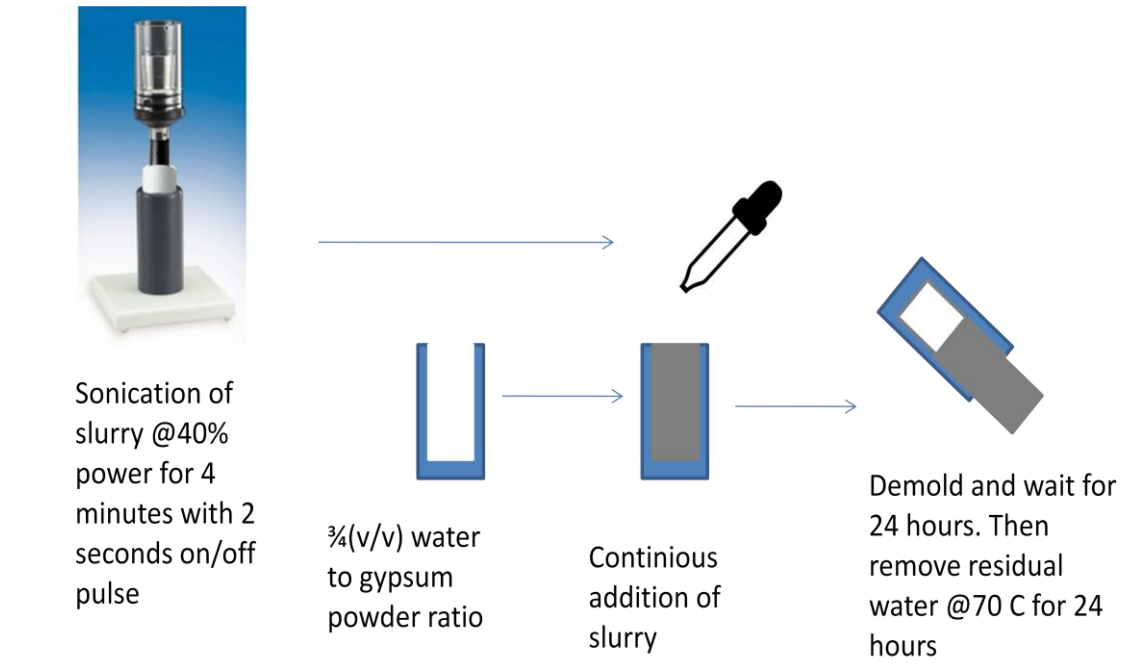


**Figure 10 Schematics of preparation of alumina green bodies**



## CHAPTER 3

### RESULTS AND DISCUSSION

#### 3. 1 Stability of suspensions

The electrokinetic behavior of 200 nm alumina particles at their native state and in the presence of the superplasticizer was investigated. This superplasticizer has both carboxylic acid groups and sulfonate groups which gradually promote more negative charge as the slurry gets more basic. Due to different dissociation constants of acrylate and sulfonate groups, the slurry stays at highly negative zeta potentials for a wide pH range. Higher dissociation constant of ionic sulfonate groups enables the superplasticizers to strongly adsorb onto positively charged alumina particles. This electrostatic interactions concert the expanded random coil configuration leading to an increased stability [21]. The isoelectric point (IEP) of alumina particles was measured to be at pH ~7.6 indicating that the surface of particles hold Al–OH bonds and positively charged sites of Al–OH<sub>2</sub><sup>+</sup> between pH 7 and 8 [15]. The zeta potential of alumina particles lay below –25 mV over a wide pH range (2–12) above 0.7 wt% addition of superplasticizer (Figure 11). We carried out the experiments in native pH levels without the adjustment of pH owing to this wide range stability.

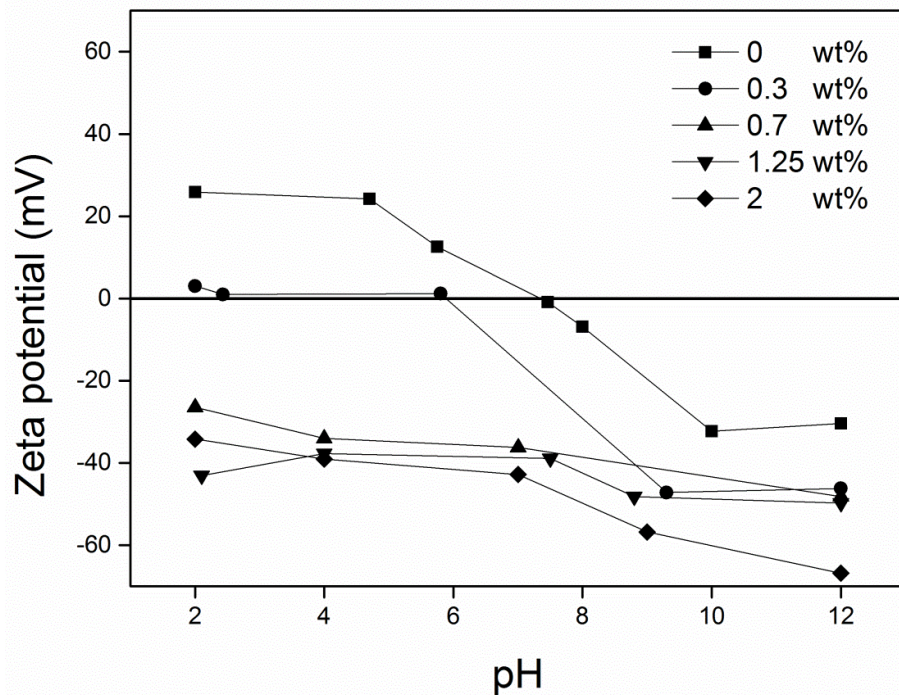


**Figure 11 Effect of pH on zeta potential of the alumina suspensions in the presence of different amounts of superplasticizer**

There are four main factors which determine the sign and amplitude of the zeta potential. First, the charged sulfonic acid and carboxylic acid groups tend to interact with charged surface of alumina particles and form salts. Second, since this polyelectrolyte is adsorbed through an ion exchange mechanism, there is an overall increase in entropy as ions are released to the media. Third, as the superplasticizers get adsorbed to the alumina surface, a loss of conformational entropy accompanies each polymer chain. Fourth, the adsorbed superplasticizer chain segments repulse each other due to unfavorable segment to segment interactions. The first two factors contribute to stabilization and an increase in net zeta potential whereas the last two decrease and devalue the zeta potential.

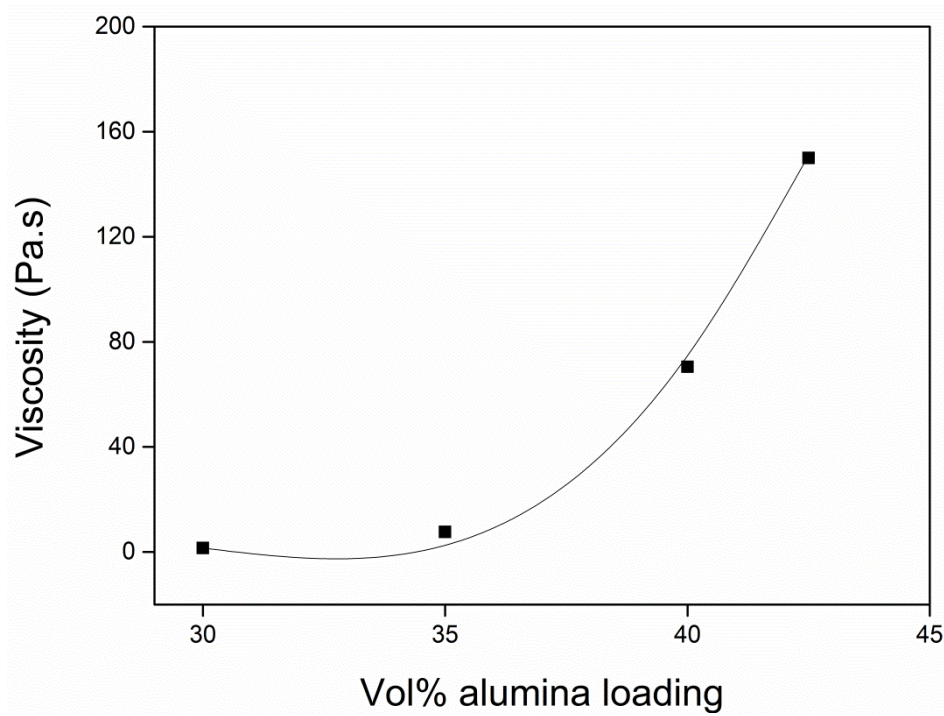
### 3. 2 Rheological measurements

Figure 13 shows the effect of alumina content on the rheological behavior of the suspensions. As the vol% alumina loading increased, the Van der Waals forces increased respectively. The flowability was almost halted for 45 vol% suspension

indicating that this point was close to maximum particle loading. Krieger and Dougherty model was used to find maximum particle loading[19]:

$$\mu = \mu_0 \left(1 - \frac{\phi}{\phi_{max}}\right)^{-\left(\frac{\mu}{\phi_{max}}\right)} \quad (1)$$

Where  $\mu$  is the viscosity of the suspension (Pa.s),  $\mu_0$  is the viscosity of the media (Pa.s),  $\phi_{max}$  is the maximum particle loading (vol%) achievable for a system. Fitting the vol% alumina loading to Krieger and Dougherty equation provides a  $\phi_{max}$  value of 45.7 vol% for our system that is consistent with the empirical measurement.



**Figure 12** Viscosity of the suspensions with different alumina loading rates at  $1s^{-1}$  shear rate

Viscosities in the range of 0.3–10 Pa.s were found to work well with solid casting and shear rates of 1–100 s<sup>-1</sup> are frequently encountered in the process [41,47–49]. Lower viscosities result in well-packed green bodies that is necessary to produce high strength structures [50]. The rotational viscosity of 35 wt% alumina suspensions in the presence of 1–4 wt% superplasticizer at the shear rate of 1 s<sup>-1</sup> was monitored.

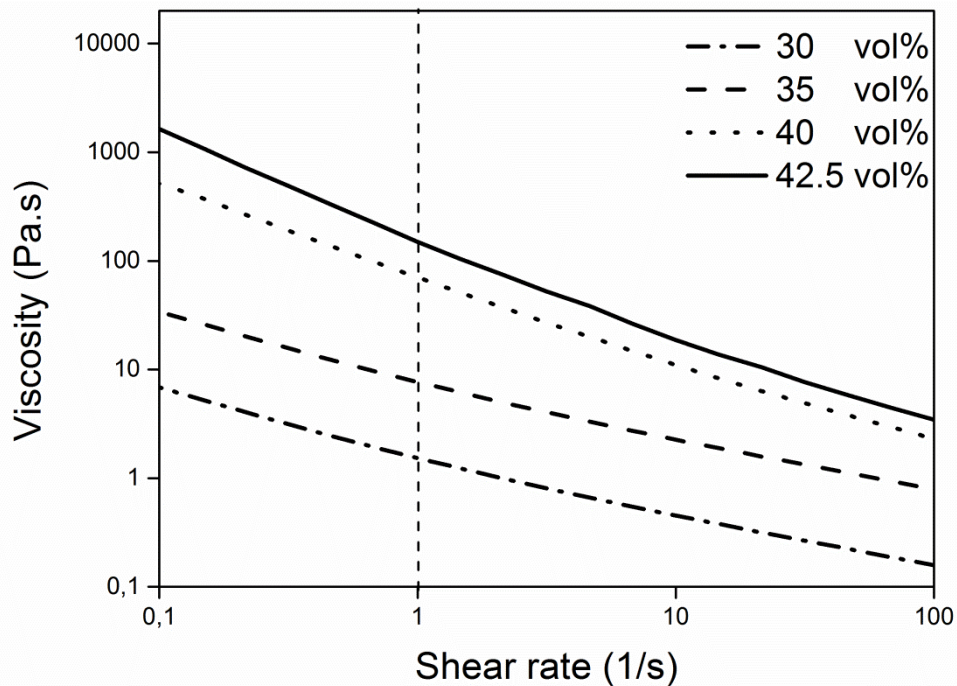


**Figure 13 Viscosity of 35 vol% alumina suspensions in the presence of 1–4 wt% superplasticizer**

A cross section elucidated the viscosity profile of the suspension shown in Figure 14. The viscosity sharply drops from 20 Pa.s to 7 Pa.s from 1 wt% superplasticizer to 1.25 wt% and then increases to 15 Pa.s for 1.5 wt%. This kind of behavior was frequently reported for PCE copolymers; Bouhamed, *et al.* investigated this phenomenon with coblock PCE superplasticizers and proposed that this dip was related to steric contribution of PEG side chains [16]. Jiang *et al.* observed similar dips in a series of PCE-based superplasticizers and correlate the trend in viscosity with ionic charge in the backbone of polymers [9]. The mechanical characterization of the green bodies was performed at 1.25 wt% superplasticizer due to the lowest viscosity experienced at this composition.

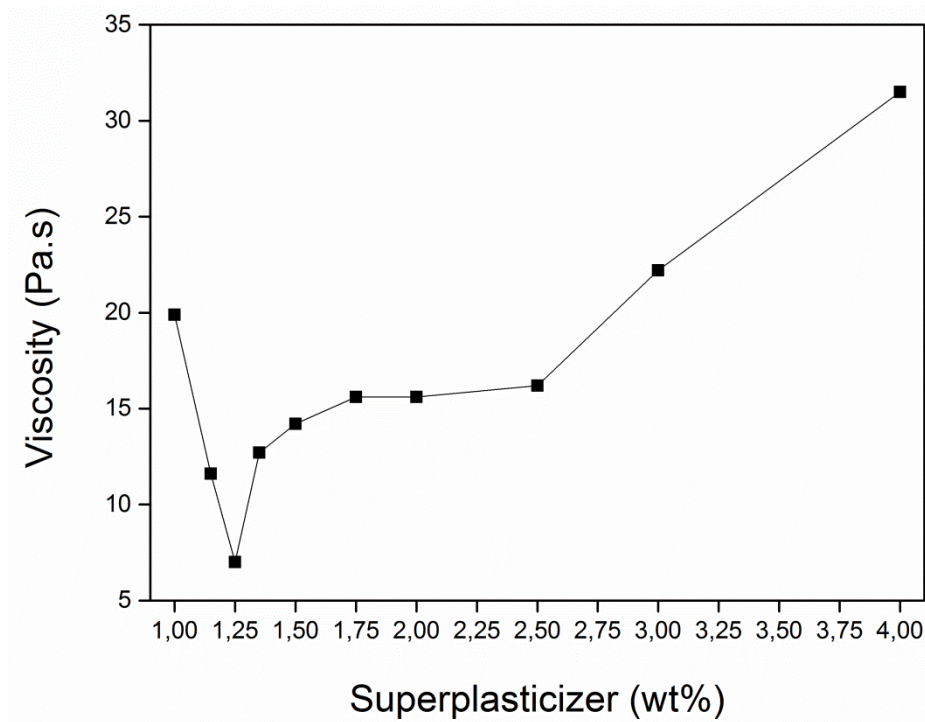


**Figure 14 Viscosity of suspensions with different amounts of superplasticizer at  $1 \text{ s}^{-1}$  shear rate**

### 3. 3 Mechanical characterization and machining of alumina green bodies

We performed the compression tests on 30–40 vol% alumina loaded samples. The compressive strength of green bodies increased with alumina loading and these results matched well with pycnometry as well (Figure 15) Although, it is desirable to have high strength green bodies, 40 vol% samples could not withstand machining speed and samples failed during the process. Therefore, we chose 35 vol% alumina to investigate green body machining.

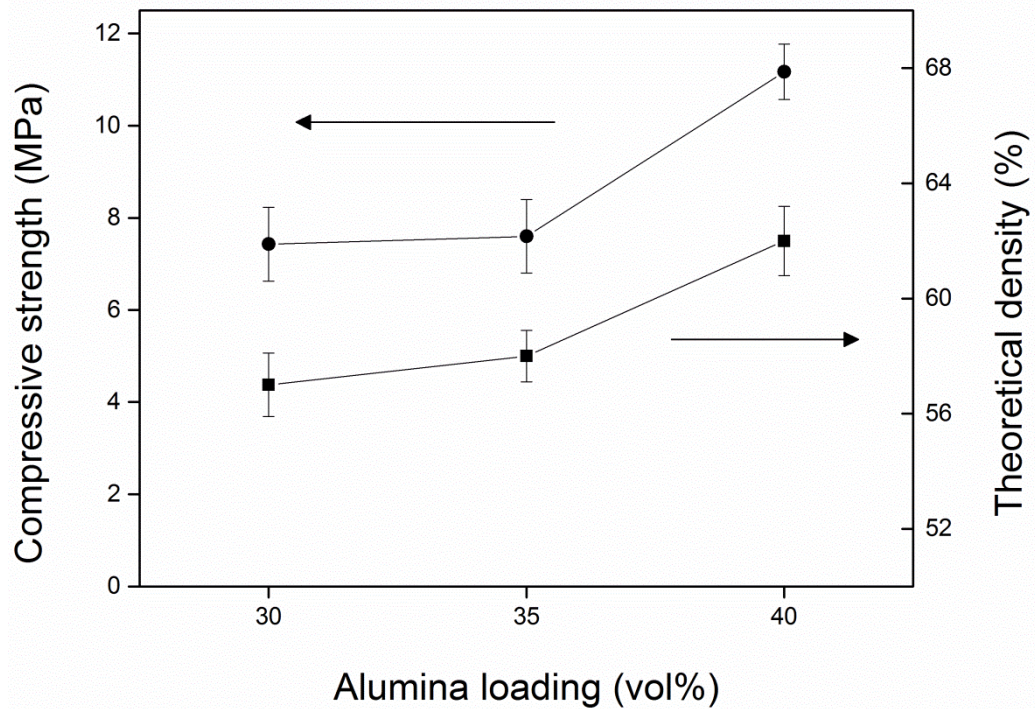


**Figure 15 Compressive strength and theoretical density of green bodies with different vol% alumina loading at 1.25 wt% superplasticizer**

Traditionally, binders such as poly(vinyl alcohol), poly(ethylene imine), poly(vinylpyrrolidone), and high molecular weight PEG were used to increase the mechanical strength of the green body for the machining processes [22,26,51]. These binders are used at least more than 4 wt% and although adding more binder contributes to the mechanical properties, it hinders the flowability of the slurry during casting [33]. In addition, there is a need for careful binder burnout procedure to prevent crack and void formation during sintering. Rheology modifiers such as poly(acrylic acid), poly(maleic acid), and Na-carboxyl methyl cellulose were utilized in the presence of binders to homogenize the slurries and have better packing. In these systems, total amount of additive can reach 4-10 wt% [13,14,52].

Through the use of 1.25 wt% superplasticizer, without any binders, we first machined the green bodies and then sintered the machined pieces without polymer burning step. The green bodies after machining are shown in Figure 16. We consistently get smooth surfaces as exemplified in Figure 17. The largest drill bit that we used had a diameter of 8.2 mm and approximately 8.3 mm holes in the green bodies with 5 mm depth. The green bodies were manufactured without visible cracks or voids. Sintered solid cast bodies shrunk  $16.1\pm 1.8\%$  at the outer diameter and  $17.5\pm 0.9\%$  at the inner diameter after sintering at 1500 °C for 2 hours.

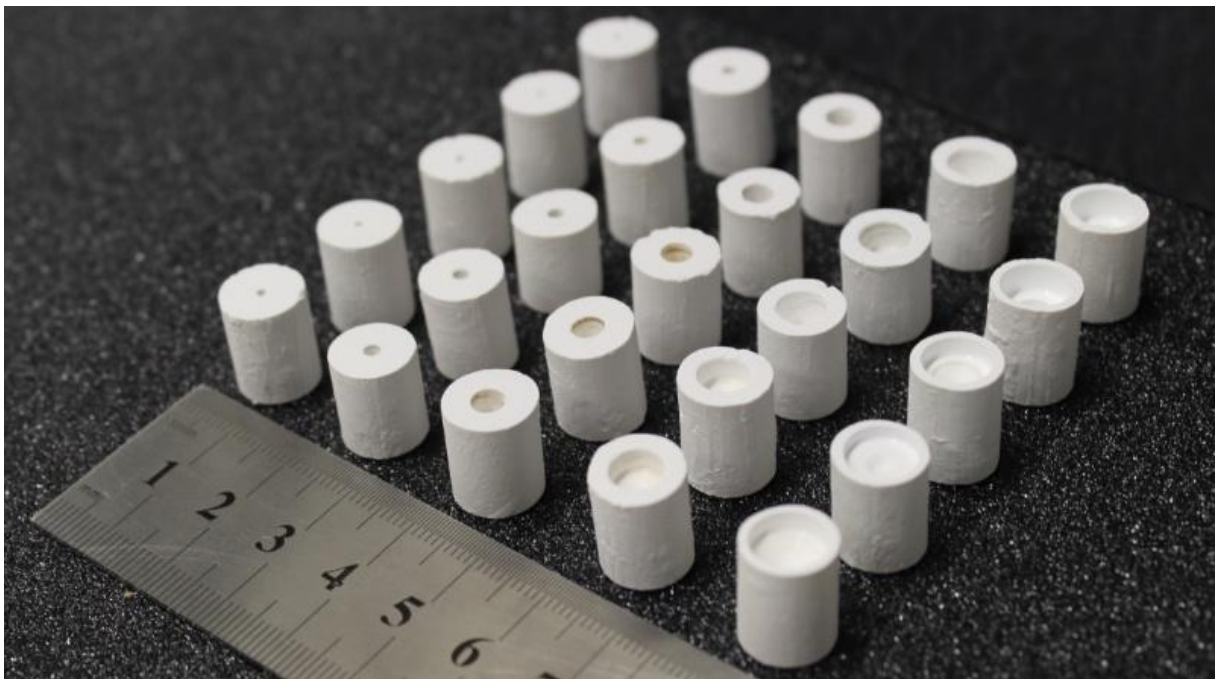


**Figure 16 From left to right: green body alumina drilled by 1.1, 2, 4, 6 and 8.2 mm drill bits. The diameters of cylinders are 10.5 mm**

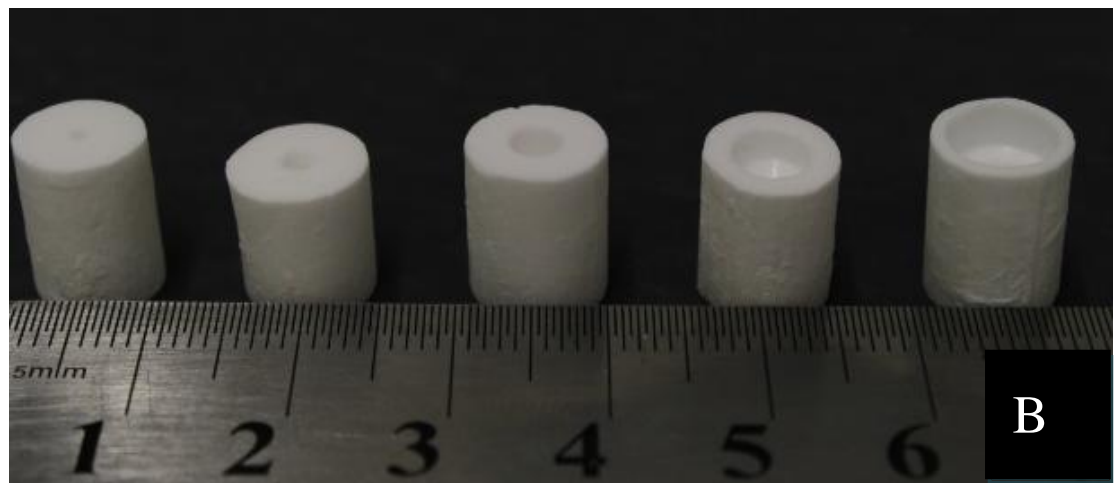
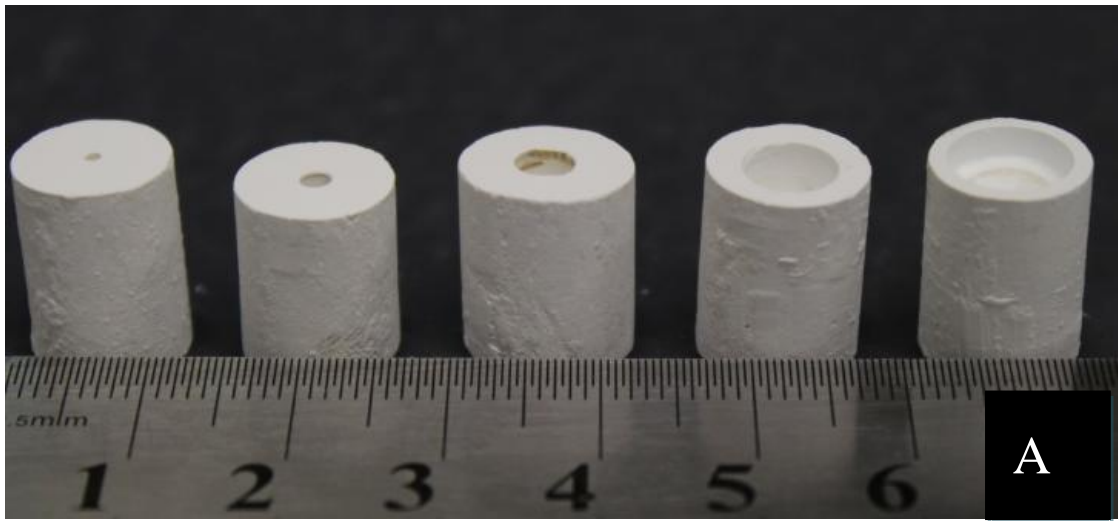
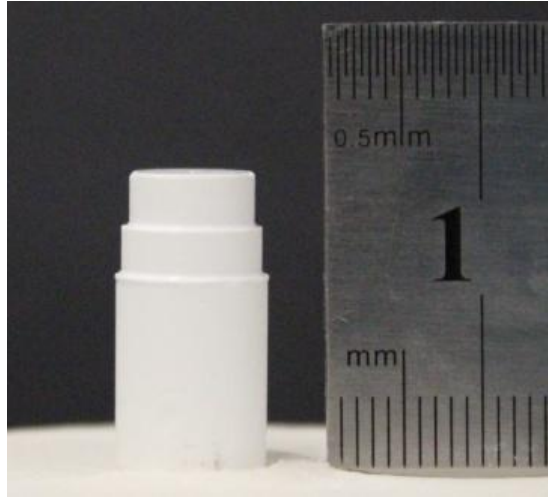
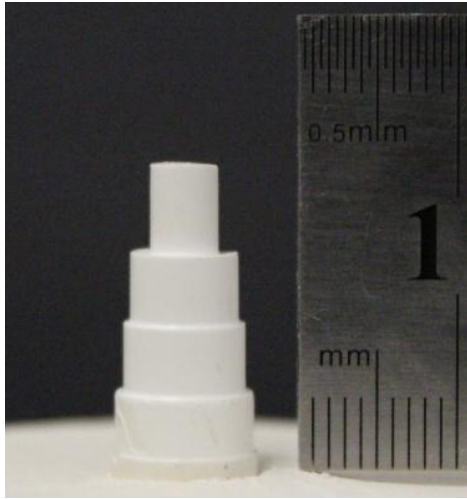




## **Figure 17 Alumina samples before (A) and after (B) sintering**

Clamping the green body to the lathe is a major problem as the green body has to be compressed until there is stability at high rotations. We used around 500-900 rpm for drilling (slower for larger holes) and 700-1200 rpm for lathing. We had to start from fresh tooling as alumina was highly abrasive. Before drilling with the planned drill head, we centered the cylindrical green body with a standard drill head. This was crucial since the tip of the drill is skewed and an initial contact with the flat alumina surface would crack the samples due to torsion forces. We observed the drilled powder could not be exhausted efficiently as drilling progressed deeper. Our hypothesis is that this initiates internal pressure to build up and increase chance of failure during machining. For 8 mm wide holes we performed the machining in two steps to prevent this internal pressure buildup. First we drilled a 6 mm wide 5 mm deep hole was drilled and got rid of the machined dust. We used a similar clamping procedure for lathing as for drilling. The circularity of the sample was more important for lathing procedure as this gradient translated into considerable forces in high speed machining. Through lathing producing stepped structures is challenging because machining forces usually produce surface cracks. Our samples produced minimal cracks and the ones that formed were mostly healed through the sintering process as nanopowders merged into grains through sintering process.

PCE superplasticizers can be utilized for fabrication of alumina green bodies. Our PCE provides sufficient mechanical strength such that green bodies can withstand drilling and lathing operations with minimal cracks and flaws. We did not detect extensive carbon burnout during machining thus eliminated the binder burnout step. We were able to achieve loadings up to 45 vol% where up to 40 vol% samples were suitable for slip casting techniques. We observed that the 35 vol% loaded samples achieved the lowest viscosity at 1.25 wt% superplasticizer addition. Increasing the superplasticizer amount at higher values where literature resided provided green bodies with higher compressive strengths but the samples became too brittle to be properly machined. Drilling operations with high aspect ratio to sample sizes were successfully provided. Up to 8 mm drill radius to 10.5 mm sample radius drilling was observed. We did not observe

carbon burnout and smoke during drilling which has been the case for studies with more binders. Since we add small amount of binder compared to similar experiments, we also encountered particle packing on the order of 58 to 62%. This high particle packing enabled good sintering without major pore entrapment. Another benefit of using low amount of binders without additional plasticizers was the complete elimination of binder burnout step. The binders were homogenously eliminated through the regular heat ramping required to sinter alumina. The superplasticizer acts as a binder, plasticizer, and deflocculant which bring new venues to slip casting of ceramics.

## **CHAPTER 4**

### **FUTURE WORK**

#### 4. 1 Robocasting

Robocasting is a free form fabrication method mainly used to cast complex 3D ceramic objects. Utilizing additive manufacturing methods, continuous filaments are deposited through a thin nozzle. To stabilize this type of ceramic suspensions, high amount of binders and viscosity modifiers are required. Figure 18 shows a robocast ceramic scaffold. As the complexity of a shape increases, the interface between building blocks determines the final mechanical integrity and strength. In robocasting, as the slurry comes out of the nozzle, it has to provide flowability but as soon as the slurry hits the substrate it has to solidify. To accommodate this property, an additional additive must be integrated to the suspension. Stress yielding behaviour at low shear rates assist the slurry to become rigid as soon as it is cast. This strategy enabled production of very thin grid network type of 3D structures and are further investigated for bioapplications [53]. Our superplasticizer can act both as binder and plasticizer thus we believe our superplasticizer can be useful in robocasting techniques.

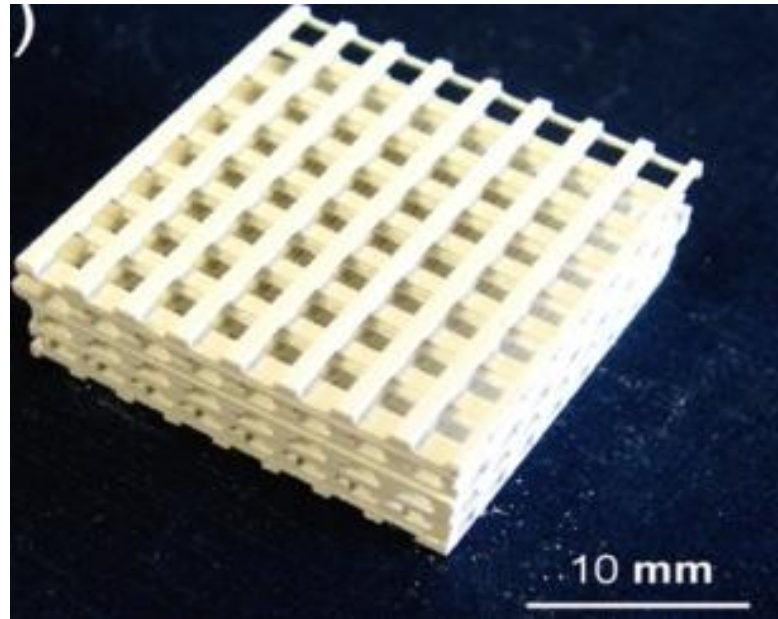


**Figure 18 Robocast green body scaffold [54]**

#### 4. 2 Inkjet printing

Inkjet printing provides fast and cheap fabrication of printed ceramics on substrates. To successfully inkjet a material, i) proper extensional viscosity, ii) homogenous binder distribution, and iii) uniform speed of ink on the substrate is required. Prasad, *et al.* investigated the inkjet printing of alumina with an oleic acid as a dispersant. Up to 15 vol% loadings were achieved with ethanol. Figure 19 shows homogenous droplet spread desired for inkjet printing [55]. Akhlaghi, *et al.* investigated the extensional viscosity of alumina in water with our superplasticizer and proposed that this system can potentially be used in inkjet printing [18]. Our superplasticizer is soluble in ethanol and similar volatile organic compounds so we believe it will behave suitable behavior for inkjet printing.

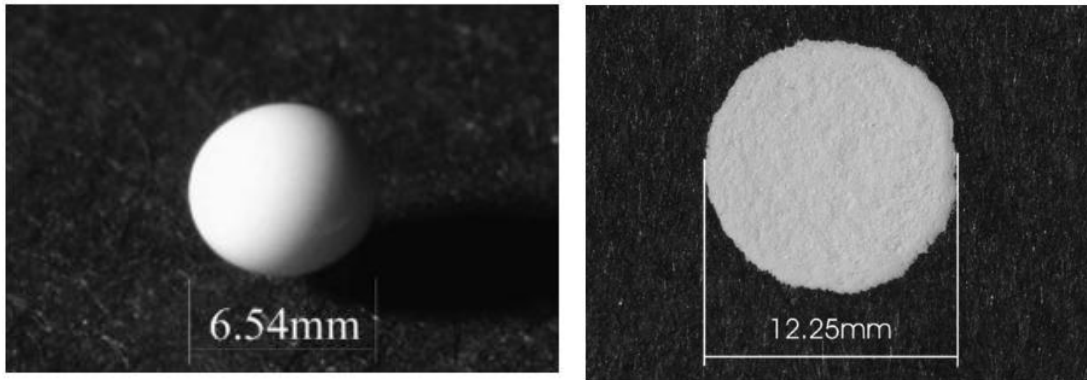


**Figure 19 Inkjet print alumina before contact and after spreading on the substrate [55]**

#### 4. 3 Hydrogen separation membranes

Due to high chemical and heat resistance of alumina, porous bodies are frequently used as ultrafiltration and gas separation membranes [28]. Hydrogen separation membranes are important for the separation industry as the hydrogen production and separation processes are unified thus lowering processing temperatures [56].  $\gamma$ -alumina cannot be used in this process as high pressure and steam can cause these phases to transform into  $\alpha$ -alumina thereby changing the properties of the structure. To get a high performance with  $\alpha$ -alumina, control of both pore size and diameter is crucial. Figure 20 illustrates an ideal hydrogen separation membrane. If single particle size is used, the minimum pore size becomes one fifth of the size of the particle. In our preliminary results we have investigated the surface structure of alumina surfaces prepared with 35 vol% loading 1.25 wt% PCE and fired in 1400 C for 2 hours. The micro-nanostructure was homogenous and can be potentially used for separation membrane applications.

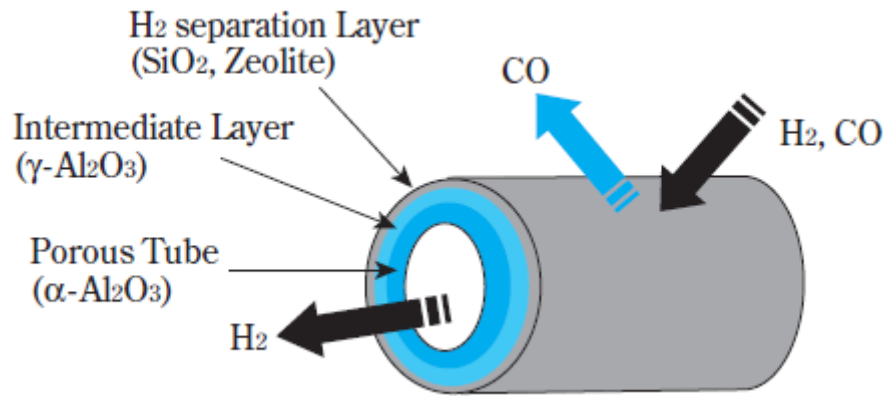


**Figure 20 Illustration of porous hydrogen separation membranes[44]**

## REFERENCES

- [1] Y. Lalatonne, J. Richardi, M.P. Pileni, Van der Waals versus dipolar forces controlling mesoscopic organizations of magnetic nanocrystals., *Nat. Mater.* 3 (2004) 121–125. doi:10.1038/nmat1054.
- [2] K. Cai, Y. Huang, J. Yang, Alumina gelcasting by using HEMA system, *J. Eur. Ceram. Soc.* 25 (2005) 1089–1093. doi:10.1016/j.jeurceramsoc.2004.04.024.
- [3] C. Tallon, M. Limacher, G. V. Franks, Effect of particle size on the shaping of ceramics by slip casting, *J. Eur. Ceram. Soc.* 30 (2010) 2819–2826. doi:10.1016/j.jeurceramsoc.2010.03.019.
- [4] P. Marco, J. Llorens, Understanding of naphthalene sulfonate formaldehyde condensates as a dispersing agent to stabilise raw porcelain gres suspensions, *Colloids Surfaces A Physicochem. Eng. Asp.* 299 (2007) 180–185. doi:10.1016/j.colsurfa.2006.11.034.
- [5] K. Yamada, T. Takahashi, S. Hanehara, M. Matsuhisa, Effects of the chemical structure on the properties of polycarboxylate-type superplasticizer, *Cem. Concr. Res.* 30 (2000) 197–207. doi:10.1016/S0008-8846(99)00230-6.
- [6] H. Byman-Fagerholm, P. Mikkola, J.B. Rosenholm, E. Lidén, R. Carlsson, The influence of lignosulphonate on the properties of single and mixed Si<sub>3</sub>N<sub>4</sub> and ZrO<sub>2</sub> suspensions, *J. Eur. Ceram. Soc.* 19 (1999) 41–48. doi:10.1016/S0955-2219(98)00162-9.
- [7] J.C. Le Bell, V.T. Hurskainen, P.J. Stenius, The influence of sodium lignosulphonates on the stability of kaolin dispersions, *J. Colloid Interface Sci.* 55 (1976) 60–68. doi:10.1016/0021-9797(76)90008-4.
- [8] Y.F. Houst, R.J. Flatt, P. Bowen, H. Hofmann, a G. Sika, Influence of superplasticizer adsorption on the rheology of cement paste, *Int. Conf. "The Role Chem. Admixtures High Perform. Concr.* 1999 (1999) 387–402. [http://infoscience.epfl.ch/record/29515/files/Monterey\\_RF\\_YH\\_99.pdf](http://infoscience.epfl.ch/record/29515/files/Monterey_RF_YH_99.pdf).
- [9] B. Jiang, S. Zhou, H. Ji, B. Liao, H. Pang, Dispersion and rheological properties of ceramic suspensions using linear polyacrylate copolymers with carboxylic groups as superplasticizer, *Colloids Surfaces A Physicochem. Eng. Asp.* 396 (2012) 310–316. doi:10.1016/j.colsurfa.2012.01.015.
- [10] H. Bouhamed, S. Boufi, a. Magnin, Dispersion of alumina suspension using comb-like and diblock copolymers produced by RAFT polymerization of AMPS and MPEG, *J. Colloid Interface Sci.* 312 (2007) 279–291. doi:10.1016/j.jcis.2007.03.060.
- [11] H. Hommer, Interaction of polycarboxylate ether with silica fume, *J. Eur. Ceram. Soc.* 29 (2009) 1847–1853. doi:10.1016/j.jeurceramsoc.2008.12.017.

- [12] A.A. Zaman, R. Tsuchiya, B.M. Moudgil, Adsorption of a Low-Molecular-Weight Polyacrylic Acid on Silica, Alumina, and Kaolin, *J. Colloid Interface Sci.* 256 (2002) 73–78. doi:10.1006/jcis.2001.7941.
- [13] A.M. Kjeldsen, R.J. Flatt, L. Bergström, Relating the molecular structure of comb-type superplasticizers to the compression rheology of MgO suspensions, *Cem. Concr. Res.* 36 (2006) 1231–1239. doi:10.1016/j.cemconres.2006.03.019.
- [14] P. Marco, J. Llorens, Surface charge and rheological properties of raw porcelain gres suspension with acrylic copolymers bearing carboxylic groups, *J. Eur. Ceram. Soc.* 29 (2009) 559–564. doi:10.1016/j.jeurceramsoc.2008.07.024.
- [15] P. Bowen, C. Carry, D. Luxembourg, H. Hofmann, Colloidal processing and sintering of nanosized transition aluminas, *Powder Tech.* 157 (2005) 100–107. doi:10.1016/j.powtec.2005.05.015.
- [16] H. Bouhamed, S. Boufi, a. Magnin, Alumina interaction with AMPS-MPEG copolymers produced by RAFT polymerization: Stability and rheological behavior, *J. Colloid Interface Sci.* 333 (2009) 209–220. doi:10.1016/j.jcis.2009.01.030.
- [17] L. Palmqvist, O. Lyckfeldt, E. Carlström, P. Davoust, A. Kauppi, K. Holmberg, Dispersion mechanisms in aqueous alumina suspensions at high solids loadings, *Colloids Surfaces A Physicochem. Eng. Asp.* 274 (2006) 100–109. doi:10.1016/j.colsurfa.2005.08.039.
- [18] O. Akhlaghi, O. Akbulut, Y. Menciloglu, Extensional rheology and stability behavior of alumina suspensions in the presence of AMPS-modified polycarboxylate ether-based copolymers, *Colloid Polym. Sci.* (2015) doi:http://dx.doi.org/10.1007/s00396-015-3683-8. doi:10.1007/s00396-015-3683-8.
- [19] A. Dörr, A. Sadiki, A. Mehdizadeh, A discrete model for the apparent viscosity of polydisperse suspensions including maximum packing fraction, *J. Rheol. (N. Y. N. Y.)* 57 (2013) 743. doi:10.1122/1.4795746.
- [20] J.J. Stickel, R.L. Powell, Fluid mechanics and rheology of dense suspensions, *Annu. Rev. Fluid Mech.* 37 (2005) 129–149.
- [21] J. Cesarano, I.A. Aksay, Processing of highly concentrated aqueous alpha-alumina suspensions stabilized with poly-electrolytes, *J. Am. Ceram. Soc.* 71 (1988) 1062–1067. doi:10.1111/j.1151-2916.1988.tb05792.x.
- [22] M. Acosta, V.L. Wiesner, C.J. Martinez, R.W. Trice, J.P. Youngblood, Effect of polyvinylpyrrolidone additions on the rheology of aqueous, highly loaded alumina suspensions, *J. Am. Ceram. Soc.* 96 (2013) 1372–1382. doi:10.1111/jace.12277.



- [23] D. Myers, Colloids and Colloidal Stability, in: Surfaces, Interfaces, and Colloids, John Wiley & Sons, Inc., 2002: pp. 214–252. <http://dx.doi.org/10.1002/0471234990.ch10>.
- [24] J.S. Reed, Principles of ceramics processing, 1995. <http://books.google.de/books?id=9hKKQgAACAAJ>.
- [25] D. Hotza, P. Greil, Review: aqueous tape casting of ceramic powders, Mater. Sci. Eng. A. 202 (1995) 206–217.
- [26] B. Nystrom, A.-L. Kjøniksen, Effects of Polymer Concentration and Cross-Linking Density on Rheology of Chemically Cross-Linked Poly(vinyl alcohol) near the Gelation Threshold, Macromolecules. 29 (1996) 5215–5222.
- [27] S. Dhara, B. Su, Green machining to net shape alumina ceramics prepared using different processing routes, Int. J. Appl. Ceram. Technol. 2 (2005) 262–270. doi:10.1111/j.1744-7402.2005.02021.x.
- [28] U.T. Gonzenbach, A.R. Studart, D. Steinlin, E. Tervoort, L.J. Gauckler, Processing of particle-stabilized wet foams into porous ceramics, J. Am. Ceram. Soc. 90 (2007) 3407–3414.
- [29] J. Yang, J. Yu, Y. Huang, Recent developments in gelcasting of ceramics, J. Eur. Ceram. Soc. 31 (2011) 2569–2591. doi:10.1016/j.jeurceramsoc.2010.12.035.
- [30] J.K. Montgomery, P.L. Drzal, K.R. Shull, K.T. Faber, Thermoreversible Gelcasting: A Novel Ceramic Processing Technique, Rheology. 1 (2002) 1164–1168.
- [31] X. Mao, S. Shimai, M. Dong, S. Wang, Gelcasting of Alumina Using Epoxy Resin as a Gelling Agent, J. Am. Ceram. Soc. 90 (2007) 986–988. doi:10.1111/j.1551-2916.2007.01492.x.
- [32] K.M. Lindqvist, E. Carlström, Indirect solid freeform fabrication by binder assisted slip casting, J. Eur. Ceram. Soc. 25 (2005) 3539–3545. doi:10.1016/j.jeurceramsoc.2004.10.013.
- [33] X. Li, Q. Li, YAG ceramic processed by slip casting via aqueous slurries, Ceram. Int. 34 (2008) 397–401. doi:10.1016/j.ceramint.2006.10.018.
- [34] J. Yu, J. Yang, Y. Huang, The transformation mechanism from suspension to green body and the development of colloidal forming, Ceram. Int. 37 (2011) 1435–1451. doi:10.1016/j.ceramint.2011.01.019.
- [35] J. Chandradass, K.H. Kim, D. sik Bae, K. Prasad, G. Balachandar, S.A. Divya, et al., Starch consolidation of alumina: Fabrication and mechanical properties, J. Eur. Ceram. Soc. 29 (2009) 2219–2224. doi:10.1016/j.jeurceramsoc.2009.02.001.

- [36] M.H. Talou, A.G.T. Martinez, M.A. Camerucci, Green mechanical evaluation of mullite porous compacts prepared by pre-gelling starch consolidation, *Mater. Sci. Eng. A*. 549 (2012) 30–37. doi:10.1016/j.msea.2012.03.111.
- [37] L. Yin, H.X. Peng, L. Yang, B. Su, Fabrication of three-dimensional inter-connective porous ceramics via ceramic green machining and bonding, *J. Eur. Ceram. Soc.* 28 (2008) 531–537. doi:10.1016/j.jeurceramsoc.2007.07.006.
- [38] T. Besshi, T. Sato, I. Tsutsui, Machining of alumina green bodies and their dewaxing, *J. Mater. Process. Technol.* 95 (1999) 133–138. doi:10.1016/S0924-0136(99)00280-0.
- [39] M.A. Janney, S.D. Nunn, C.A. Walls, O.O. Omatete, R.B. Ogle, G.H. Kirby, et al., *Gelcasting, Handb. Ceram. Eng.* (1998) 1–15.
- [40] A. Kaşgöz, Z. Özbaş, H. Kaşgöz, I. Aydın, Effects of monomer composition on the mechanical and machinability properties of gel-cast alumina green compacts, *J. Eur. Ceram. Soc.* 25 (2005) 3547–3552. doi:10.1016/j.jeurceramsoc.2004.09.013.
- [41] S. Mohanty, A.P. Rameshbabu, S. Mandal, B. Su, S. Dhara, Critical issues in near net shape forming via green machining of ceramics: A case study of alumina dental crown, *J. Asian Ceram. Soc.* 1 (2013) 274–281. doi:10.1016/j.jascer.2013.06.005.
- [42] K. Prabhakaran, C. Pavithran, Gelcasting of alumina from acidic aqueous medium using acrylic acid, *J. Eur. Ceram. Soc.* 20 (2000) 1115–1119. doi:10.1016/S0955-2219(99)00244-7.
- [43] K. Prabhakaran, C. Pavithran, M. Brahmakumar, S. Ananthakumar, Gelcasting of alumina using urea-formaldehyde: III. Machinable green bodies by copolymerization with acrylic acid, *Ceram. Int.* 27 (2001) 185–189. doi:10.1016/S0272-8842(00)00061-4.
- [44] B. Chemicals, *Development of New High-Purity Alumina*, (2007) 1–10.
- [45] I. Chen, X. Wang, Sintering dense nanocrystalline ceramics without final-stage grain growth, *Nature*. 404 (2000) 168–71. doi:10.1038/35004548.
- [46] P. Oyewole, SalamiZhou, Johann, Synthesis, effectiveness, and working mechanism of humic acid-{sodium 2-acrylamido-2-methylpropane sulfonate-co-N,N-dimethyl acrylamide-co-acrylic acid} graft copolymer as high-temperature fluid loss additive in oil well cementing, *J. Appl. Polym. Sci.* 126 (2012) 1449–1460. doi:10.1002/app.
- [47] R.G. Neves, B. Ferrari, a. J. Sanchez-Herencia, C. Pagnoux, E. Gordo, Role of stabilisers in the design of Ti aqueous suspensions for pressure slip casting, *Powder Technol.* 263 (2014) 81–88. doi:10.1016/j.powtec.2014.04.093.

- [48] M. Li, P. Gehre, C.G. Aneziris, Investigation of calcium zirconate ceramic synthesized by slip casting and calcination, *J. Eur. Ceram. Soc.* 33 (2013) 2007–2012. doi:10.1016/j.jeurceramsoc.2013.02.010.
- [49] M.B. Kakade, D. Das, S. Ramanathan, Studies on slip casting behavior of lanthanum strontium manganite, *Ceram. Int.* 37 (2011) 1789–1793. doi:10.1016/j.ceramint.2011.01.044.
- [50] S. Leo, C. Tallon, G. V. Franks, Aqueous and Nonaqueous Colloidal Processing of Difficult-to-Densify Ceramics: Suspension Rheology and Particle Packing, *J. Am. Ceram. Soc.* 97 (2014) 3807–3817. doi:10.1111/jace.13220.
- [51] M.E. Seitz, W.R. Burghardt, K.T. Faber, K.R. Shull, Acrylic triblock copolymer gels for thermoreversible gelcasting of ceramics, *Abstr. Pap. 233rd ACS Natl. Meet. Chicago, IL, United States, March 25-29, 2007.* (2007) POLY-488.
- [52] C.F. Alamaki, M.B. Eyhaghi, Slip casting process for the manufacture of tubular alumina microfiltration membranes, 27 (2009).
- [53] J.N. Stuecker, J. Cesarano, D. a. Hirschfeld, Control of the viscous behavior of highly concentrated mullite suspensions for robocasting, *J. Mater. Process. Technol.* 142 (2003) 318–325. doi:10.1016/S0924-0136(03)00586-7.
- [54] P. Miranda, A. Pajares, E. Saiz, A.P. Tomsia, F. Guiberteau, Mechanical properties of calcium phosphate scaffolds fabricated by robocasting, *J. Biomed. Mater. Res. - Part A.* 85 (2008) 218–227. doi:10.1002/jbm.a.31587.
- [55] P.S.R.K. Prasad, A.V. Reddy, P.K. Rajesh, P. Ponnambalam, K. Prakasan, Studies on rheology of ceramic inks and spread of ink droplets for direct ceramic ink jet printing, *J. Mater. Process. Technol.* 176 (2006) 222–229. doi:10.1016/j.jmatprotec.2006.04.001.
- [56] J.Z. Li, T. Wu, Z.Y. Yu, L. Zhang, G.Q. Chen, D.M. Guo, Micro machining of pre-sintered ceramic green body, *J. Mater. Process. Technol.* 212 (2012) 571–579. doi:10.1016/j.jmatprotec.2011.10.030.